NIH Public Access
Author Manuscript
Cancer Res. Author manuscript; available in PMC 2011 October 15.

Published in final edited form as:
Cancer Res. 2010 October 15; 70(20): 8127–8137. doi:10.1158/0008-5472.CAN-09-4613.

Epithelial-to-mesenchymal transition promotes tubulin detyrosination and microtentacles that enhance endothelial engagement

Rebecca A. Whipple[1], **Michael A. Matrone**[1,2], **Edward H. Cho**[1,2], **Eric M. Balzer**[1,2], **Michele I. Vitolo**[1], **Jennifer R. Yoon**[1,2], **Olga B. Ioffe**[1,4], **Kimberly C. Tuttle**[1,4], **Jing Yang**[5], and **Stuart S. Martin**[1,2,3]

[1]Marlene and Stewart Greenebaum NCI Cancer Center, University of Maryland School of Medicine, 655 W. Baltimore St., Baltimore, MD 21201, USA

[2]Program in Molecular Medicine, University of California, San Diego, 9500 Gilman Drive, La Jolla,CA 92093, USA

[3]Department of Physiology, University of California, San Diego, 9500 Gilman Drive, La Jolla,CA 92093, USA

[4]Department of Pathology, University of California, San Diego, 9500 Gilman Drive, La Jolla,CA 92093, USA

[5]Department of Pharmacology and Pediatrics, School of Medicine, University of California, San Diego, 9500 Gilman Drive, La Jolla,CA 92093, USA

Abstract

Epithelial-to-mesenchymal transition (EMT) is associated with increased breast tumor metastasis, but the specific mechanisms by which EMT promotes metastasis remain somewhat unclear. Despite the importance of cytoskeletal dynamics during both EMT and metastasis, very few current studies examine the cytoskeleton of detached and circulating tumor cells. Specific post-translational α-tubulin modifications are critical for adherent cell motility and implicated in numerous pathologies, but also remain understudied in detached cells. We report here that EMT induced through ectopic expression of Twist or Snail promotes α-tubulin detyrosination and the formation of tubulin-based microtentacles in detached human mammary epithelial cells. Mechanistically, EMT downregulates tubulin tyrosine ligase enzyme resulting in an accumulation of detyrosinated α-tubulin (Glu-tubulin), and increases microtentacles that penetrate endothelial layers to facillitate tumor cell reattachment. Confocal microscopy demonstrates that microtentacles are capable of penetrating the junctions between endothelial cells. Suppression of endogenous Twist in metastatic human breast tumor cells is capable of reducing both tubulin detyrosination and microtentacles. Clinical breast tumor samples display high concordance between Glu-tubulin and Twist expression levels, emphasizing the coupling between EMT and tubulin detyrosination *in vivo*. Coordinated elevation of Twist and Glu-tubulin at invasive tumor fronts, particularly within ductal carcinoma in situ samples, establishes that EMT-induced tubulin detyrosination occurs at the earliest stages of tumor invasion. These data support a novel model where the EMT that occurs during tumor invasion downregulates tubulin tyrosine ligase, increasing α-tubulin detyrosination and promoting microtentacles which could enhance the reattachment of circulating tumor cells to the vascular endothelium during metastasis.

Corresponding author: Dr. Stuart S. Martin, Bressler Bldg. Rm 10-29, 655 W. Baltimore St., Baltimore, MD 21201, Tel: 410-706-6601, Fax: 410-706-6600, ssmartin@som.umaryland.edu.

NIH-PA Author Manuscript
NIH-PA Author Manuscript
NIH-PA Author Manuscript

NIH-PA Author Manuscript
NIH-PA Author Manuscript
NIH-PA Author Manuscript

Introduction

During metastasis, tumor cells respond to the changing microenvironment with internal adaptations that are reflected in the cytoskeleton. Investigating how cytoskeletal alterations provide selective advantages to tumor cells could identify new therapeutic targets to reduce metastasis. Recently, attention has focused on the complex transition that differentiated epithelial cells undergo into a mesenchymal state and its involvement in tumor progression (1–3). Activation of this epithelial-to-mesenchymal transition (EMT) has been implicated as a means by which cancer cells can overcome the physical constraints of the primary tumor to become motile, invade surrounding tissue, and enter the vasculature (3, 4). It is also worth considering whether the molecular programs that tumor cells execute in response to the changing microenvironment could influence the metastatic potential of circulating tumor cells.

While there is significant research detailing the mechanisms involved with intravasation and the later stages of extravasation (5), the mechanism by which disseminated tumor cells reattach to the endothelium is poorly understood. Recent advances in intravital imaging have enabled direct observation and experimental manipulation of circulating cells *in vivo* (6, 7). Compelling intravital imaging shows that microtubule (MT) destabilizing compounds prevent adhesion of circulating colon carcinoma cells to the vascular endothelium (8). While the functional role of MTs during initial tumor cell reattachment *in vivo* remains undetermined, we recently identified MT-based membrane protrusions (termed microtentacles) that frequently occur on detached breast carcinoma cell lines which exhibit mesenchymal phenotypes (9, 10). Microtentacles (McTNs) are supported by the mesenchymal-associated intermediate filament protein, vimentin, and also detyrosinated α-tubulin (Glu-tubulin), a post-translational cleavage of the c-terminal tyrosine on α-tubulin (11). Stabilization of MTs induces detyrosination that can inhibit MT disassembly (12), and detyrosinated-MTs can persist for as long as 16h in cells while dynamic tyrosinated-MTs typically persist for only 3–5 minutes (11). Restoration of the c-terminal tyrosine on α-tubulin is mediated by the tubulin tyrosine ligase (TTL) enzyme. Recent live-cell imaging in adherent fibroblasts show that most MTs depolymerize upon contact with the cell membrane; however, MTs in TTL knock-out fibroblasts persist significantly longer at the membrane with an increased time spent growing (12). Interestingly, TTL suppression has been reported to provide a selective advantage during tumor growth (13) and the resulting tubulin detyrosination has been associated with poor prognosis in patients (14).

Membrane McTNs in detached cells have been previously shown to be supported by detyrosinated MTs in coordination with vimentin intermediate filaments (9, 10). These structural features, and the observation that McTNs are strongly enhanced by actin-disrupting agents, establish McTNs as novel cytoskeletal structures that are mechanistically-distinct from traditional actin-based protrusions such as filopodia, invadopodia, and podosomes (15). Perturbation of McTNs with tubulin-depolymerizing agents, vimentin-targeted phosphatase inhibitors, or expression of dominant-negative vimentin significantly reduces both the frequency of McTNs and cellular reattachment to extracellular matrix (10, 16). Furthermore, MT-stabilizing compounds enhance adhesion and McTN frequency in detached breast carcinoma cells (17).

Given the increased McTN frequency in mesenchymal breast carcinoma cell lines, we chose to examine the incidence of McTNs in immortalized human mammary epithelial cells (HMLE) that have undergone a regulated EMT via stable Twist or Snail expression (18, 19). Furthermore, we investigated the effects of suppressing endogenous Twist expression. We report here that EMT downregulates expression of TTL enzyme in HMLEs leading to elevated tubulin detyrosination and increased incidence of McTNs. Suppression of

NIH-PA Author Manuscript

NIH-PA Author Manuscript

NIH-PA Author Manuscript

endogenous Twist reduced the frequency of McTNs and decreased the expression level and organization of Glu-tubulin. Moreover, a clear concordance between Twist expression and Glu-tubulin is observed in matched serial sections of patient tumors, reinforcing our observations *in vivo*. HMLE Twist and Snail lines attach at a significantly increased rate when suspended over a human bone marrow endothelial (HBME) layer and confocal microscopy captures McTN extension to facilitate attachment and stabilization. Our results identify a novel regulatory mechanism within the EMT program that influences the post-translational modification of α-tubulin, promoting McTN extension that enhances reattachment of breast tumor cells to endothelial cells.

Materials and Methods

Cell Culture

HMLEs stably expressing GFP, Twist, or Snail (50) were grown in MEGM media kit (Lonza) at 37°C in 5% CO_2. MDA-MB-157 obtained from American Type Culture Collection (Manassas, VA) were maintained in L-15 (Gibco) containing 10% fetal bovine serum (FBS), penicillin-streptomycin (100μg/ml), and L-glutamine (2mmol/L) at 37°C without CO_2. HBME cells were provided by Antonio Passaniti (UMGCC) and grown in DMEM (Gibco) containing 10% FBS, penicillin-streptomycin (100μg/mL each) and L-glutamine (2mM) at 37°C in 5% CO_2. Cell line authentication procedures described in supplementary data.

Live Cell Imaging and Microtentacle Scoring

Live cell imaging and McTN scoring were previously described (10). Since the HMLE vector control is GFP+, we used CellMask-Orange membrane stain (Invitrogen, manufacturer's protocol). For each trial, at least 100 single cells were scored blindly for McTNs after 30min in suspension and counted positive when two or more protrusions extended greater than the radius of the cell body. Live cell imaging used an Olympus CKX41 inverted fluorescence microscope (Melville, NY).

Indirect Immunofluorescence

For suspended cell immunofluorescence, HMLE-GFP, Twist, and Snail cells were detached in serum-free media for 30min and fixed as previously described (10). For attached cell experiments, sub-confluent HMLE-GFP, Twist, and Snail as well as MDA-MB-157 cells were fixed in 3.7% formaldehyde/PBS (10min, room temp).

Immunostaining used mouse monoclonal antibodies: vimentin clone V9 (1:1000; Zymed) and twist1 (1:250; abCam), and rabbit polyclonal anti-detyrosinated tubulin (Glu; 1:500; Chemicon). Secondary detection was with Alexa-568 conjugated anti-IgG and Hoescht-33342 (1:5000; Sigma) for DNA.

Western Blot

Sub-confluent HMLE-GFP, Twist, Snail and MDA-MB-157 were washed in PBS then harvested as previously described (10). Total protein (20μg) was separated on a 4–12% NuPage MES Bis-Tris gradient gel (Invitrogen) then transferred to Immuno-Blot PVDF membranes (Bio-Rad, Hercules, CA). Monoclonal E-cadherin (1:500; BD Biosciences), vimentin clone V9 (1:1000; Zymed), twist1 (1:250; abCam), α-tubulin DM1A (1:2000; Sigma), and β-Actin (1:2000; AC-15, Sigma). Polyclonal detyrosinated tubulin (1:1000; Chemicon) and N-cadherin (1:500; Cell Signaling) and snail (1:250; Cell Signaling) were used. Secondary ECL+ chemiluminescent detection was with HRP-conjugated anti-IgG antibodies (1:5000; GE Healthcare, Piscataway, NJ). Rabbit polyclonal TTL antibody described in supplementary methods.

NIH-PA Author Manuscript

NIH-PA Author Manuscript

NIH-PA Author Manuscript

Cell-electrode Impedance Attachment Assay

Real-time, dynamic monitoring of cell-substratum attachment was measured utilizing the xCelligence RTCA-SP real-time cell sensing device (Roche) to compare the attachment rates of the HMLE GFP vector control, Twist, and Snail. HMLE cells (10,000) were seeded in triplicate into 96-well microelectronic sensored standard plates (E-plates). Attachment was expressed as a change in cell index (CI), an arbitrary unit reflecting the relative change in electrical impedance from cell-electrode interaction across microelectronic sensor arrays. Electrical impedance was measured for 0.1 sec. every 5min for a duration of 75min. Values are the mean+/−S.D. of triplicate wells (3 independent trials).

HMLE Attachment and Microtentacle Engagement to Human Bone Marrow Endothelial Layer

HMLE-GFP, Twist, and Snail cell lines were stained with calcein-AM (0.5μg/ml) (Invitrogen). Cells were detached with enzyme-free cell dissociation solution, resuspended in growth media and 50,000 cells were plated over confluent HBME layers at 37°C. At 1h, the attached cells were washed with fresh growth media. Fluorescence was measured using a Biotek SynergyHT microplate reader (Excitation:485nm, Emission:528nm). Attachment was calculated as the fluorescent signal after aspirating the media divided by the fluorescent signal from duplicate wells that were not aspirated. Values shown are mean+S.D. (eight independent trials). Confocal imaging detailed in Supplementary Methods.

Patient Samples and Immunohistochemistry

Ten fresh/frozen patient breast tumor tissue samples obtained by surgery or biopsy from the UMGCC Pathology Biorepository and Research Core as well as a human breast cancer TMA (US BioMax, Rockville, MD; #BR961) containing 33 cases of invasive ductal breast carcinoma and 13 cases of normal and non-malignant breast tissue were examined. TMA sections were deparaffinized, rehydrated and epitope retrieval heat-induced (DakoTRS, S1699/1700), followed by endogenous peroxidase blocking with hydrogen peroxide. All sections were incubated with the primary antibody Twist (1:250; H-81, Santa Cruz) or detyrosinated tubulin (1:150; Chemicon) overnight. Diaminobenzidine detection was performed on an automatic stainer using EnVision+ (DAKO). The staining intensity of Twist and Glu-tubulin was scored independently and blindly for each section according to 4 categories: negative-0; weak-1; moderate-2; and strong-3. Samples with ±1 histological scores and staining within matching cells were scored as "concordant". When staining intensity differed by at least two histological scores (0–2 or 1–3) or within different cells, the sample was scored as "discordant" staining.

Results

Induction of EMT by Twist or Snail expression promotes microtentacle formation in detached human mammary epithelial cells

To investigate the role that EMT plays in McTN formation in detached cells, HMLEs ectopically expressing the Twist or Snail transcription factors were analyzed and compared to a GFP-expressing vector control HMLE line. Adherent HMLE cells expressing Twist or Snail display a characteristic mesenchymal morphology compared to the vector control cells (Figure 1A – top panels), including the loss of cell-cell contacts, cell scattering, and reduced apical-basal cell polarity (18, 19).

Given the morphological alterations observed in adherent cells, we investigated the incidence of McTNs in detached cells that have undergone EMT. HMLE cells were fluorescently labeled with CellMask. Following 30min of suspension, HMLE Twist or Snail displayed extensive, motile McTNs compared to the control cell line (Figure 1A – lower

NIH-PA Author Manuscript

NIH-PA Author Manuscript

NIH-PA Author Manuscript

panels). Blinded quantitative analysis (Figure 1B) revealed significantly higher McTN frequencies in the suspended HMLEs expressing Twist (15-fold) or Snail (20-fold) compared to the vector control cells ($P \leq 0.005$; n=6, 3 independent trials).

Evaluation of hallmark EMT markers via Western blot supports the transition from epithelial to mesenchymal states. The protein expression profile illustrates E-Cadherin to N-Cadherin switch, vimentin expression, and both Twist and Snail upregulation in the respective transformed lines (Figure 1C). Given the increased McTN frequency in HMLE lines that have transitioned to a mesenchymal state and our previous studies showing detyrosinated tubulin enrichment that support McTNs, the HMLE lines were also evaluated for Glu-tubulin expression. Interestingly, the HMLE lines that expressed Twist or Snail also exhibited higher levels of Glu-tubulin that were linked to decreased expression of tubulin tyrosine ligase (TTL) enzyme compared to the control epithelial HMLE (Figure 1D).

HMLE Twist and Snail have increased organization of detyrosinated microtubules

Glu-tubulin organization is a key determinant of cellular asymmetry during directional cell migration (20) and can induce abnormal cell morphology (21). We further investigated the organization of elevated Glu-tubulin in HMLE Twist and Snail lines. Immunofluorescence revealed weak cytoplasmic staining with minimal Glu-enriched MTs in the HMLE control cell line; however, HMLE Twist and Snail cells formed an elaborate network of Glu-tubulin filaments, including extensive bundling in elongated regions of the cell (Figure 2A).

Since McTNs are supported by Glu-tubulin (10), we examined whether the HMLE Twist and Snail lines demonstrated Glu-tubulin increases following detachment that could promote McTNs (Figure 2B). The HMLE vector control line continued to show a weak cytoplasmic staining for Glu-tubulin, consistent with the low percentage of McTNs observed in live cell suspension. Conversely, the HMLE Twist and Snail lines displayed elevated Glu-tubulin levels throughout the cell body and McTNs. Confocal imaging of suspended cells shows that the MT network remains detectable and contains a subpopulation of Glu-MTs that can extend into the McTNs (Figure S1).

Suppressing endogenous expression of Twist in MDA-MB-157 reduces detyrosinated microtubule organization and McTN occurrence

Given the striking increase in Glu-MT organization following EMT, we examined the reverse effect of suppressing endogenous Twist on cytoskeletal morphology. We targeted Twist based on epistasis experiments illustrating that Twist acts upstream of Snail (22). The MDA-MB-157 cell line was selected because it originated from a metastatic carcinoma, exhibits high Twist mRNA levels ((23); data not shown), and displays a BasalB/mesenchymal phenotype ((9); Figure S2). In addition, MDA-MB-157s displayed the highest level of McTNs among a panel of breast carcinomas (10). Immunofluorescence also confirms that MDA-MB-157s have elevated Glu-tubulin and McTNs containing Glu-tubulin (Figure S1).

MDA-MB-157s were transfected with Twist siRNA and evaluated after four days. Western blot analysis showed a significant decrease in Twist expression compared to the non-silencing (NS) control siRNA (Figure 3A). Notably, Glu-tubulin expression levels also decreased when endogenous Twist was suppressed. Other EMT hallmarks were unaffected, suggesting that Twist suppression alone did not invoke reversion to an epithelial state through mesenchymal-to-epithelial transition (MET). This further indicates that Glu-tubulin is an early target in the Twist pathway, occurring upstream of events such as reinstatement of E-cadherin and downregulation of vimentin when EMT-associated transcription factors are suppressed (24).

NIH-PA Author Manuscript

NIH-PA Author Manuscript

NIH-PA Author Manuscript

Glu-tubulin organization was also altered when Twist was silenced in MDA-MB-157s. The characteristic nuclear localization of the Twist transcription factor was decreased and delocalized after 4 days of Twist siRNA, compared to a nonsilencing control (Figure 3B, a and d). MDA-MB-157s display filamentous networks of Glu-MTs and suppression of Twist decreased filamentous Glu-tubulin, likely through decreased MT stability (Figure 3B, b and e). While reducing endogenous Twist significantly decreased the expression and organization of Glu-tubulin in the MDA-MB-157s, vimentin appeared unaffected (Figure 3B, c and f).

Since Glu-tubulin expression and organization decreased following Twist suppression, we investigated the effects of Twist silencing on McTNs. MDA-MB-157s in which Twist, and subsequently Glu-tubulin, was downregulated with Twist siRNA (4d) displayed a significantly lower frequency of McTNs (53%) compared to control NS cells (75%), a 29% overall decrease in McTN occurrence (Figure 3C).

Concordance of Detyrosinated Tubulin and Twist in Invasive Breast Tumors

Given the coupling of Twist and Glu-tubulin *in vitro*, we examined patient samples on parallel tissue microarrays with serial matched core sections. Normal breast epithelial ducts stain weakly for both Twist and Glu, while the cancerous region invading the normal duct displayed stronger staining (Figure 4A- a and d). Two independent tumor tissue cores from 33 patients (n=66) with invasive ductal carcinoma (IDC) were analyzed blindly for Twist and Glu staining. A significant majority of IDC samples displayed similar staining intensities for Glu and Twist and concordance between Glu and Twist (measured as ±1 histological scores) accounted for 95% of the IDC samples (63/66). Further examination revealed that the same cells within the serial sections stained for both Glu and Twist (Figure 4A- b and e; white arrows). When staining intensity differed by at least two histological scores (0–2 or 1–3) or within different cells, the sample was scored as "discordant" (Figure 4A- c and f; black arrows), and was only observed in 5% of the IDC samples (3/66). There were varying staining intensities noted between different cores from the same patient, indicating heterogeneity of Twist and Glu expression within a given tumor. Tumor heterogeneity has implicated the surrounding microenvironment itself as an essential regulatory mechanism for EMT (2).

To examine the tumor microenvironment more extensively, larger sections of breast tumors including adjoining normal tissue were obtained from UMGCC tissue repository. Low magnification revealed that both Twist and Glu stained heavily at the invasive tumor front flanking normal stroma (Figure 4B – a and d). Higher magnification showed strong staining of the invasive front (Figure 4B - b and e) compared to the tumor center that displayed weak staining in both Glu and Twist (Figure 4B – c and f). Tumor sections from patients with ductal carcinoma in situ establish that Twist and Glu are coordinately upregulated at the earliest stages of invasion at the tumor front (Figure 4C, black arrows). Conversely, in the later stages of tumor invasion, tumor cells that remain together as “nests” suppress both Twist and Glu (Figure S3).

Epithelial-to- Mesenchymal Transition promotes cell reattachment

We compared the reattachment efficiency of HMLE cells to those expressing Twist or Snail using real-time electrical impedance monitoring as well as fluorescent detection over a confluent endothelial layer. The detailed impedance time-course (25), shows that HMLE Twist and Snail cells attached at significantly faster rates than the HMLE vector control line (Figure 5A and Figure S4). Most strikingly, HMLE-Twist reattached 8-fold more than HMLE vector control cells at 30 minutes.

NIH-PA Author Manuscript

NIH-PA Author Manuscript

NIH-PA Author Manuscript

HMLE variants stained with calcein-AM were also analyzed during reattachment to confluent monolayers of human bone marrow endothelial (HBME) cells (Figure 5B). The HMLE Twist and Snail again reattached more efficiently than vector control cells ($P \leq 0.005$; n=8; t-test). Representative images captured at 1h also illustrate the difference in attachment (Figure 5C). The majority of HMLE vector control cells retained a rounded morphology, while the HMLE Twist and Snail showed significantly more cells attached and spread on the HBME layer.

HMLE Twist and Snail attachment is facilitated by McTNs

In order to capture McTNs during the process of attachment, GFP-Membrane transfected cells were suspended over a confluent layer of HMBEs expressing mCherry and fixed after 20 minutes. Confocal images of these early stages of endothelial attachment are presented from a top, side, and angled view to visualize McTN orientation (Figure 6). HMLE vector control cells remain rounded without any observable McTNs at all viewing angles. The top view of HMLE Twist or Snail shows numerous McTNs protruding from the cell (white arrows). Angled and side views when the endothelial fluorescence signal is computationally removed demonstrate that McTNs penetrate the endothelial layer to contact the underlying surface and McTNs on the apical surface bend towards the HBME layer. Surface renderings also show specific penetrations at endothelial cell junctions (Figure S5). Interestingly, the distal ends of these McTNs are rounded and our previous research shows that this rounded end contains actin (16), similar to neurite growth cones or sites of integrin clustering (26).

Discussion

In the present study, we demonstrate that activation of the EMT program via Twist or Snail expression significantly increases α-tubulin detyrosination by downregulating TTL and alters microtubule stability and organization to promote plasma-membrane microtentacles in detached cells. This mechanism extends to metastatic human breast tumor cells, where the detyrosination and reorganization of microtubules depend on endogenous Twist expression. Microtubule stability and subsequent tubulin detyrosination, are more sensitive to changes in endogenous Twist expression than the more well-known effects on vimentin and cadherin expression, indicating that microtubule alterations are a primary effect of EMT. Both tissue microarrays and larger tissue sections from breast cancer patients demonstrate that Twist expression occurs concurrently with tubulin detyrosination *in vivo*, particularly at the invasive front where tumor cells move through adjacent tissue. Microtentacles induced by Twist or Snail promote cell reattachment and confocal microscopy demonstrates penetration of endothelial cell layers by microtentacles. This evidence supports a model where the EMT program induced in malignant cells during movement through surrounding tissue produces specific microtubule alterations that promote McTNs and could provide a selective advantage during metastatic tumor cell reattachment.

Normal epithelial cells have a highly structured, rigid cytoskeletal network that is incompatible with cell motility (27). Acquisition of mesenchymal features induces an elongated, front-to-back polarized morphology which supports single cell migration (2). The dynamic cytoskeletal properties and greater deformability of transformed cells support successful metastasis (28, 29). While actin rearrangement during EMT has been increasingly studied (27), there has been limited investigation of EMT-induced microtubule alterations. Both the mesenchymal intermediate filament vimentin and Glu-tubulin influence cell migration, promote McTNs and indicate poor patient prognosis (14, 30–32) presenting a compelling case to investigate MT alterations that occur during EMT.

While EMT was first described in embryogenesis (33, 34), the similarities recently observed in cancer pathology (35, 36) and tumor stem cell phenotypes (19) suggest that epithelial

NIH-PA Author Manuscript

NIH-PA Author Manuscript

NIH-PA Author Manuscript

cells possess an inherent capacity to transform in response to activating cues. Increases in Glu-enriched stable MTs have been reported during differentiation and implicated in generating cell asymmetry to direct migration (20, 37). Interestingly, rapid Glu-tubulin accumulation has been reported during the early stages of myogenesis when cultured myoblasts are placed in differentiation media (38). Inhibition of tubulin detyrosination prevented morphogenesis (39), suggesting a Glu-dependent mechanism for morphological transformations. Additionally, tubulin detyrosination in TTL-deficient cells yielded morphological perturbations, producing large membrane extensions in adherent cells, and abnormalities in cell polarization (21). While such morphological changes are required for development, they are potentially detrimental to cancer patients. Stabilization of MTs, which elevates tubulin detyrosination (40), is regulated by factors such as microtubule-associated proteins (MAPs) or plus end-binding proteins such as CLIP-170, EB1, and Cap-Gly (21, 41). The tubulin tyrosination/detyrosination cycle occurs through the interchange of an unidentified tubulin carboxypeptidase (TCP) that enzymatically removes the carboxy-terminal tyrosine residue of α-tubulin, exposing a glutamate (Glu), and TTL that re-incorporates the tyrosine residue (42–45). Our lab recently showed that metastatic breast cancers express the MT-stabilizing MAP protein Tau, which induces McTNs, increases reattachment of suspended cells, and retention of CTCs in lung capillaries (46). Accumulating evidence also shows that increased persistence and stability of detyrosinated microtubules could contribute to tumor metastasis. Suppression of TTL frequently occurs during tumor progression and the accumulation of Glu-tubulin predicts tumor aggressiveness (13, 14, 31, 32). Additional investigations demonstrating increased persistence and growth of MTs at the membrane in TTL-deficient cells (12), destabilization of cortical actin during an EMT (27), and compensatory rearrangements of stabilized MTs after F-actin architecture is compromised (17), support an important cytoskeletal interplay that could contribute to tubulin detyrosination, McTN formation and cancer invasiveness. Therefore, both TTL and TCP have become attractive therapeutic targets due to the connection between microtubule stability and carcinogenesis. Our present data demonstrate that EMT alters microtubules by downregulating TTL, increasing Glu-tubulin levels of stabilized MTs. Testing how EMT affects the TCP enzyme is currently unfeasible, since the TCP gene remains unidentified despite over 30 years of effort.

The selective advantage that EMT could provide cancer cells once disseminated into the lymphatics or bloodstream is of significant interest. While Twist suppression in highly metastatic 4T1 cells did not affect primary tumor formation, it significantly reduced the presence of tumor cells in the bloodstream, ultimately reducing the formation of metastatic lung nodules (18). Together with pathology studies showing Twist expression highest at invasive tumor fronts (47–49), these data suggest that Twist promotes invasion into the stroma surrounding the primary tumor but is not required for tumor growth. . Our clinical data illustrate a high concordance of Twist and Glu-tubulin localization in human IDCs with the strongest expression at the invasive front, supporting a functional link between EMT and MT stabilization. Confocal imaging data that tubulin-based McTNs penetrate endothelial layers during HMLE reattachment provide a mechanism to explain the *in vivo* findings that circulating tumor cell reattachment is inhibited by targeting tubulin polymerization (8).

The data presented here support a novel model in which EMT suppresses TTL and promotes MT stability, resulting in tubulin detyrosination and the formation of McTNs that support endothelial attachment. Cancer cells could exploit this EMT-mediated MT stabilization during escape from the primary tumor and subsequent invasion through the surrounding stroma. Since tumor cells can arrive in distant tissues within minutes of being released from the primary site, even transient changes in microtubule stability at the invasive front could significantly impact metastatic efficiency. This model is reinforced by the observations that circulating tumor cells depend on microtubules to attach on blood vessel walls (8) and our

NIH-PA Author Manuscript

NIH-PA Author Manuscript

NIH-PA Author Manuscript

findings here that tubulin microtentacles promote endothelial penetration and tumor cell reattachment. Given the role of detyrosinated tubulin in cell motility and orientation, the EMT-induced microtubule alterations we report may occur as part of an inherent program for cell movement during development, but one that also primes tumor cells for metastatic success by stabilizing microtubules and promoting microtentacles.

Supplementary Material

Refer to Web version on PubMed Central for supplementary material.

Abbreviations

HMLE	Immortalized human mammary primary epithelial cells
McTN	microtentacle
HBME	human bone marrow endothelial cell
MT	microtubule
EMT	epithelial-to-mesenchymal transition
Glu	detyrosinated tubulin
TCP	tubulin carboxypeptidase
TTL	tubulin tyrosine ligase
TMA	tissue microarray
UMGCC	University of Maryland Greenebaum Cancer Center
IDC	invasive ductal carcinoma
NS	non-silencing

Acknowledgments

Grant support: R01-CA124704 from National Cancer Institute, Breast Cancer Idea Award from USA Medical Research and Materiel Command (BC061047) and a Komen investigator-initiated research grant (KG100240).

References

1. Hugo H, Ackland ML, Blick T, Lawrence MG, Clements JA, Williams ED, Thompson EW. Epithelial--mesenchymal and mesenchymal--epithelial transitions in carcinoma progression. J Cell Physiol. 2007; 213:374–383. [PubMed: 17680632]
2. De Wever O, Pauwels P, De Craene B, Sabbah M, Emami S, Redeuilh G, Gespach C, Bracke M, Berx G. Molecular and pathological signatures of epithelial-mesenchymal transitions at the cancer invasion front. Histochem Cell Biol. 2008; 130:481–494. [PubMed: 18648847]
3. Polyak K, Weinberg RA. Transitions between epithelial and mesenchymal states: acquisition of malignant and stem cell traits. Nat Rev Cancer. 2009; 9:265–273. [PubMed: 19262571]
4. Kalluri R, Weinberg RA. The basics of epithelial-mesenchymal transition. J Clin Invest. 2009; 119:1420–1428. [PubMed: 19487818]
5. Chiang AC, Massague J. Molecular basis of metastasis. N Engl J Med. 2008; 359:2814–2823. [PubMed: 19109576]
6. Condeelis J, Segall JE. Intravital imaging of cell movement in tumours. Nat Rev Cancer. 2003; 3:921–930. [PubMed: 14737122]
7. Kedrin D, Gligorijevic B, Wyckoff J, Verkhusha VV, Condeelis J, Segall JE, van Rheenen J. Intravital imaging of metastatic behavior through a mammary imaging window. Nat Methods. 2008; 5:1019–1021. [PubMed: 18997781]

NIH-PA Author Manuscript

NIH-PA Author Manuscript

NIH-PA Author Manuscript

8. Korb T, Schluter K, Enns A, Spiegel HU, Senninger N, Nicolson GL, Haier J. Integrity of actin fibers and microtubules influences metastatic tumor cell adhesion. Exp Cell Res. 2004; 299:236–247. [PubMed: 15302590]
9. Neve RM, Chin K, Fridlyand J, Yeh J, Baehner FL, Fevr T, Clark L, Bayani N, Coppe JP, Tong F, Speed T, Spellman PT, DeVries S, Lapuk A, Wang NJ, Kuo WL, Stilwell JL, Pinkel D, Albertson DG, Waldman FM, McCormick F, Dickson RB, Johnson MD, Lippman M, Ethier S, Gazdar A, Gray JW. A collection of breast cancer cell lines for the study of functionally distinct cancer subtypes. Cancer Cell. 2006; 10:515–527. [PubMed: 17157791]
10. Whipple RA, Balzer EM, Cho EH, Matrone MA, Yoon JR, Martin SS. Vimentin filaments support extension of tubulin-based microtentacles in detached breast tumor cells. Cancer Res. 2008; 68:5678–5688. [PubMed: 18632620]
11. Webster DR, Gundersen GG, Bulinski JC, Borisy GG. Differential turnover of tyrosinated and detyrosinated microtubules. Proc Natl Acad Sci U S A. 1987; 84:9040–9044. [PubMed: 3321065]
12. Peris L, Wagenbach M, Lafanechere L, Brocard J, Moore AT, Kozielski F, Job D, Wordeman L, Andrieux A. Motor-dependent microtubule disassembly driven by tubulin tyrosination. J Cell Biol. 2009; 185:1159–1166. [PubMed: 19564401]
13. Lafanechere L, Courtay-Cahen C, Kawakami T, Jacrot M, Rudiger M, Wehland J, Job D, Margolis RL. Suppression of tubulin tyrosine ligase during tumor growth. J Cell Sci. 1998; 111(Pt 2):171–181. [PubMed: 9405300]
14. Mialhe A, Lafanechere L, Treilleux I, Peloux N, Dumontet C, Bremond A, Panh MH, Payan R, Wehland J, Margolis RL, Job D. Tubulin detyrosination is a frequent occurrence in breast cancers of poor prognosis. Cancer Res. 2001; 61:5024–5027. [PubMed: 11431336]
15. Yamaguchi H, Pixley F, Condeelis J. Invadopodia and podosomes in tumor invasion. Eur J Cell Biol. 2006; 85:213–218. [PubMed: 16546563]
16. Whipple RA, Cheung AM, Martin SS. Detyrosinated microtubule protrusions in suspended mammary epithelial cells promote reattachment. Exp Cell Res. 2007; 313:1326–1336. [PubMed: 17359970]
17. Balzer EM, Whipple RA, Cho EH, Matrone MA, Martin SS. Antimitotic chemotherapeutics promote adhesive responses in detached and circulating tumor cells. Breast Cancer Res Treat. 2009
18. Yang J, Mani SA, Donaher JL, Ramaswamy S, Itzykson RA, Come C, Savagner P, Gitelman I, Richardson A, Weinberg RA. Twist, a master regulator of morphogenesis, plays an essential role in tumor metastasis. Cell. 2004; 117:927–939. [PubMed: 15210113]
19. Mani SA, Guo W, Liao MJ, Eaton EN, Ayyanan A, Zhou AY, Brooks M, Reinhard F, Zhang CC, Shipitsin M, Campbell LL, Polyak K, Brisken C, Yang J, Weinberg RA. The epithelial-mesenchymal transition generates cells with properties of stem cells. Cell. 2008; 133:704–715. [PubMed: 18485877]
20. Gundersen GG, Bulinski JC. Selective stabilization of microtubules oriented toward the direction of cell migration. Proc Natl Acad Sci U S A. 1988; 85:5946–5950. [PubMed: 3413068]
21. Peris L, Thery M, Faure J, Saoudi Y, Lafanechere L, Chilton JK, Gordon-Weeks P, Galjart N, Bornens M, Wordeman L, Wehland J, Andrieux A, Job D. Tubulin tyrosination is a major factor affecting the recruitment of CAP-Gly proteins at microtubule plus ends. J Cell Biol. 2006; 174:839–849. [PubMed: 16954346]
22. Smit MA, Geiger TR, Song JY, Gitelman I, Peeper DS. A Twist-Snail axis critical for TrkB-induced EMT-like transformation, anoikis resistance and metastasis. Mol Cell Biol. 2009
23. Blick T, Widodo E, Hugo H, Waltham M, Lenburg ME, Neve RM, Thompson EW. Epithelial mesenchymal transition traits in human breast cancer cell lines. Clin Exp Metastasis. 2008; 25:629–642. [PubMed: 18461285]
24. Kwok WK, Ling MT, Lee TW, Lau TC, Zhou C, Zhang X, Chua CW, Chan KW, Chan FL, Glackin C, Wong YC, Wang X. Up-regulation of TWIST in prostate cancer and its implication as a therapeutic target. Cancer Res. 2005; 65:5153–5162. [PubMed: 15958559]
25. Atienza JM, Yu N, Kirstein SL, Xi B, Wang X, Xu X, Abassi YA. Dynamic and label-free cell-based assays using the real-time cell electronic sensing system. Assay Drug Dev Technol. 2006; 4:597–607. [PubMed: 17115930]

NIH-PA Author Manuscript

NIH-PA Author Manuscript

NIH-PA Author Manuscript

26. Lowery LA, Van Vactor D. The trip of the tip: understanding the growth cone machinery. Nat Rev Mol Cell Biol. 2009; 10:332–343. [PubMed: 19373241]
27. Yilmaz M, Christofori G. EMT, the cytoskeleton, and cancer cell invasion. Cancer Metastasis Rev. 2009; 28:15–33. [PubMed: 19169796]
28. Raz A, Geiger B. Altered organization of cell-substrate contacts and membrane-associated cytoskeleton in tumor cell variants exhibiting different metastatic capabilities. Cancer Res. 1982; 42:5183–5190. [PubMed: 7139623]
29. Guck J, Schinkinger S, Lincoln B, Wottawah F, Ebert S, Romeyke M, Lenz D, Erickson HM, Ananthakrishnan R, Mitchell D, Kas J, Ulvick S, Bilby C. Optical deformability as an inherent cell marker for testing malignant transformation and metastatic competence. Biophys J. 2005; 88:3689–3698. [PubMed: 15722433]
30. Domagala W, Lasota J, Dukowicz A, Markiewski M, Striker G, Weber K, Osborn M. Vimentin expression appears to be associated with poor prognosis in node-negative ductal NOS breast carcinomas. Am J Pathol. 1990; 137:1299–1304. [PubMed: 1701960]
31. Soucek K, Kamaid A, Phung AD, Kubala L, Bulinski JC, Harper RW, Eiserich JP. Normal and prostate cancer cells display distinct molecular profiles of alpha-tubulin posttranslational modifications. Prostate. 2006; 66:954–965. [PubMed: 16541425]
32. Kato C, Miyazaki K, Nakagawa A, Ohira M, Nakamura Y, Ozaki T, Imai T, Nakagawara A. Low expression of human tubulin tyrosine ligase and suppressed tubulin tyrosination/detyrosination cycle are associated with impaired neuronal differentiation in neuroblastomas with poor prognosis. Int J Cancer. 2004; 112:365–375. [PubMed: 15382060]
33. Hay ED. An overview of epithelio-mesenchymal transformation. Acta Anat (Basel). 1995; 154:8–20. [PubMed: 8714286]
34. Hay ED. The mesenchymal cell, its role in the embryo, and the remarkable signaling mechanisms that create it. Dev Dyn. 2005; 233:706–720. [PubMed: 15937929]
35. Guarino M, Rubino B, Ballabio G. The role of epithelial-mesenchymal transition in cancer pathology. Pathology. 2007; 39:305–318. [PubMed: 17558857]
36. Yang J, Weinberg RA. Epithelial-mesenchymal transition: at the crossroads of development and tumor metastasis. Dev Cell. 2008; 14:818–829. [PubMed: 18539112]
37. Onishi K, Higuchi M, Asakura T, Masuyama N, Gotoh Y. The PI3K-Akt pathway promotes microtubule stabilization in migrating fibroblasts. Genes Cells. 2007; 12:535–546. [PubMed: 17397400]
38. Gundersen GG, Khawaja S, Bulinski JC. Generation of a stable, posttranslationally modified microtubule array is an early event in myogenic differentiation. J Cell Biol. 1989; 109:2275–2288. [PubMed: 2681230]
39. Chang W, Webster DR, Salam AA, Gruber D, Prasad A, Eiserich JP, Bulinski JC. Alteration of the C-terminal amino acid of tubulin specifically inhibits myogenic differentiation. J Biol Chem. 2002; 277:30690–30698. [PubMed: 12070174]
40. Webster DR, Gundersen GG, Bulinski JC, Borisy GG. Assembly and turnover of detyrosinated tubulin in vivo. J Cell Biol. 1987; 105:265–276. [PubMed: 3301867]
41. Zhang T, Zaal KJ, Sheridan J, Mehta A, Gundersen GG, Ralston E. Microtubule plus-end binding protein EB1 is necessary for muscle cell differentiation, elongation and fusion. J Cell Sci. 2009; 122:1401–1409. [PubMed: 19366726]
42. Gundersen GG, Khawaja S, Bulinski JC. Postpolymerization detyrosination of alpha-tubulin: a mechanism for subcellular differentiation of microtubules. J Cell Biol. 1987; 107:251–264. [PubMed: 2886509]
43. Webster DR, Modesti NM, Bulinski JC. Regulation of cytoplasmic tubulin carboxypeptidase activity during neural and muscle differentiation: characterization using a microtubule-based assay. Biochemistry. 1992; 31:5849–5856. [PubMed: 1610827]
44. Wehland J, Weber K. Turnover of the carboxy-terminal tyrosine of alpha-tubulin and means of reaching elevated levels of detyrosination in living cells. J Cell Sci. 1987; 88(Pt 2):185–203. [PubMed: 2826509]
45. Barra HS, Arce CA, Argarana CE. Posttranslational tyrosination/detyrosination of tubulin. Mol Neurobiol. 1988; 2:133–153. [PubMed: 3077315]

NIH-PA Author Manuscript

NIH-PA Author Manuscript

NIH-PA Author Manuscript

46. Matrone MA, Whipple RA, Thompson K, Cho EH, Vitolo MI, Balzer EM, Yoon JR, Ioffe OB, Tuttle KC, Tan M, Martin SS. Metastatic breast tumors express increased tau, which promotes microtentacle formation and the reattachment of detached breast tumor cells. Oncogene. 29:3217–3227. [PubMed: 20228842]

47. Fendrich V, Waldmann J, Feldmann G, Schlosser K, Konig A, Ramaswamy A, Bartsch DK, Karakas E. Unique expression pattern of the EMT markers Snail, Twist and E-cadherin in benign and malignant parathyroid neoplasia. Eur J Endocrinol. 2009; 160:695–703. [PubMed: 19176646]

48. Usami Y, Satake S, Nakayama F, Matsumoto M, Ohnuma K, Komori T, Semba S, Ito A, Yokozaki H. Snail-associated epithelial-mesenchymal transition promotes oesophageal squamous cell carcinoma motility and progression. J Pathol. 2008; 215:330–339. [PubMed: 18491351]

49. Hlubek F, Brabletz T, Budczies J, Pfeiffer S, Jung A, Kirchner T. Heterogeneous expression of Wnt/beta-catenin target genes within colorectal cancer. Int J Cancer. 2007; 121:1941–1948. [PubMed: 17631641]

50. Elenbaas B, Spirio L, Koerner F, Fleming MD, Zimonjic DB, Donaher JL, Popescu NC, Hahn WC, Weinberg RA. Human breast cancer cells generated by oncogenic transformation of primary mammary epithelial cells. Genes Dev. 2001; 15:50–65. [PubMed: 11156605]

NIH-PA Author Manuscript
NIH-PA Author Manuscript
NIH-PA Author Manuscript

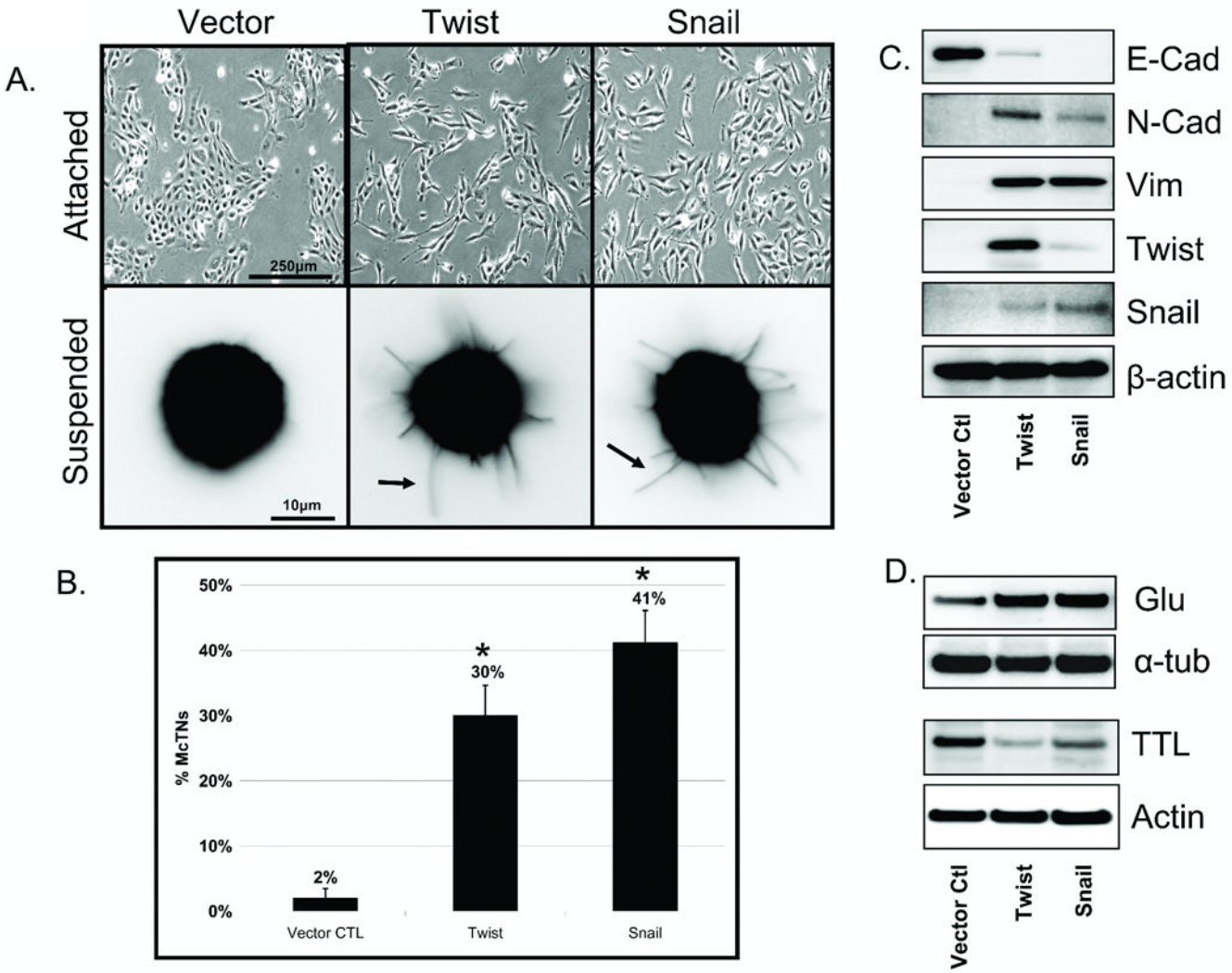

Figure 1. EMT promotes increased McTNs and tubulin detyrosination in detached HMLEs

A: Phase contrast images of attached HMLE Twist and Snail cells compared to HMLE-GFP (top panel). Detached HMLE Twist and Snail display extensive membrane McTNs (lower panel, *black arrows*). **B:** Populations of live, detached HMLE Twist and Snail cells display significantly higher McTN frequencies than HMLE-GFP cells. *Columns*, mean for six experiments, in which at least 100 CellMask stained cells were counted; *bars*, SD. ($P \leq 0.005$, *t*-test, *black asterisks*). **C:** Comparative expression profile of HMLE (GFP Vector Ctl, Twist, Snail) including E-cadherin, N-cadherin, vimentin, Twist, Snail, and β-actin as a loading control showing mesenchymal hallmarks in Twist and Snail HMLEs. **D:** HMLE Twist and Snail have increased Glu-tubulin levels and decreased levels of tubulin tyrosine ligase (TTL) compared to the HMLE-GFP while total α-tubulin and actin are comparable.

NIH-PA Author Manuscript
NIH-PA Author Manuscript
NIH-PA Author Manuscript

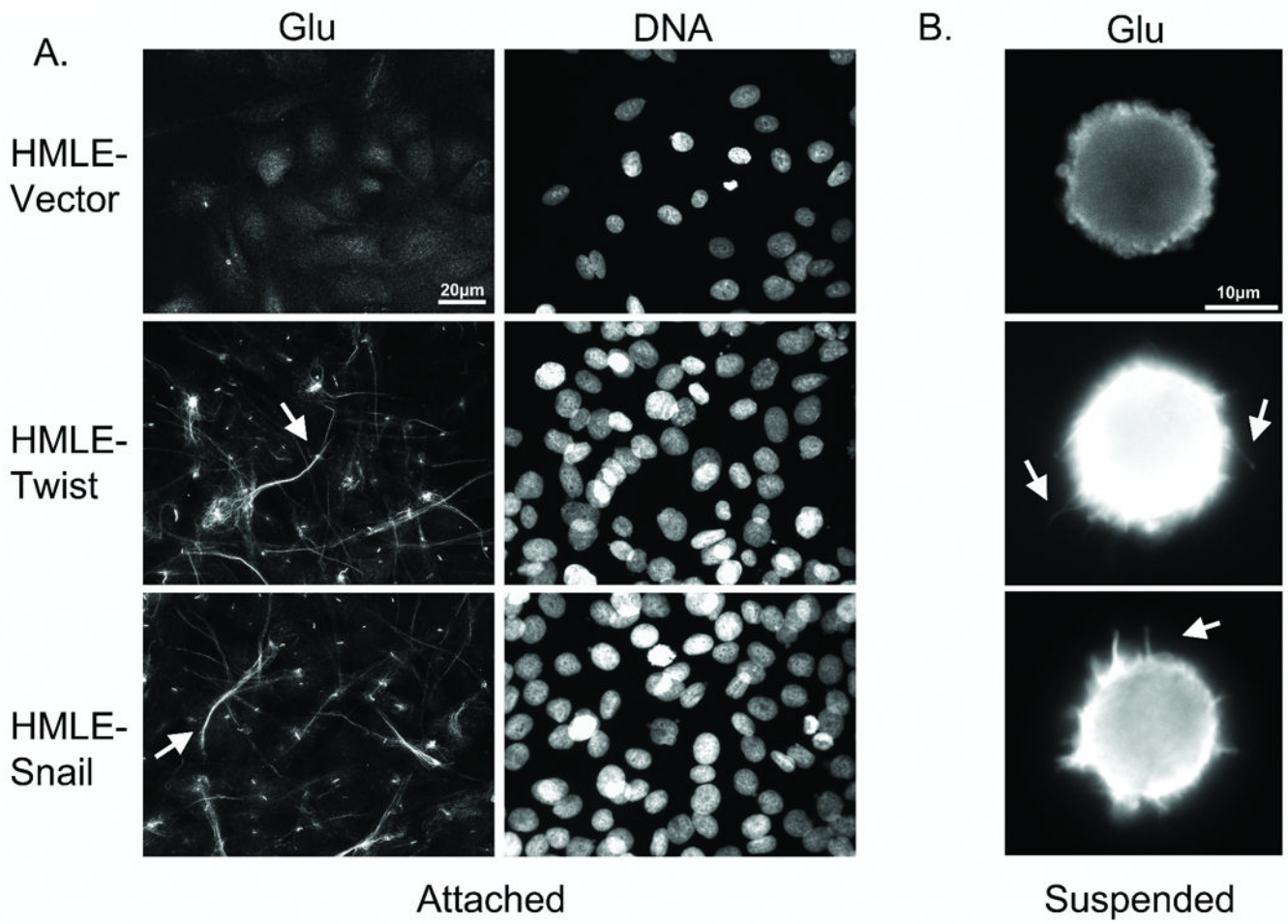

Figure 2. Glu-tubulin accumulation and reorganization during EMT

A: Attached HMLE-GFP ctl shows weak Glu staining while the HMLE Twist and Snail display filamentous accumulation and bundling of Glu-tubulin (arrows). Hoescht (d–f) was used to visualize nuclei. **B:** Detached cells were fixed and spun onto glass coverslips. Immunostaining indicates Glu-tubulin localization in HMLE Twist and Snail McTNs (*white arrows*).

NIH-PA Author Manuscript

NIH-PA Author Manuscript

NIH-PA Author Manuscript

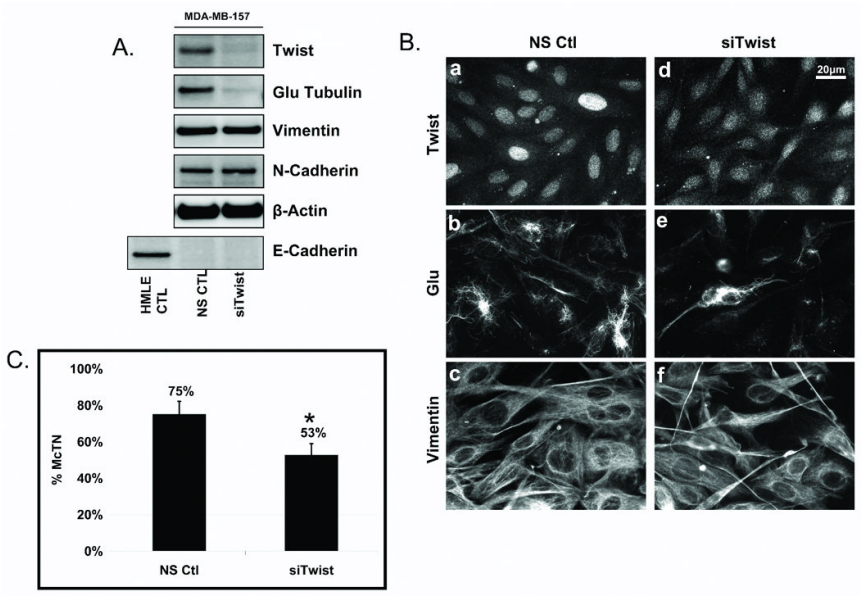

Figure 3. Endogenous Twist suppression in MDA-MB-157s decreases Glu expression and organization

A: Transfection of a non-silencing control (NS ctl) or Twist siRNA (siTwist) in MDA-MB-157s shows suppression of Twist resulted in decreased Glu-tubulin levels. Vimentin and N-cadherin remained unchanged and E-cadherin repression persisted. HMLE-GFP was used as a positive control for E-cadherin expression and β-actin was used as a loading control. **B:** Following Twist suppression in MDA-MB-157s, nuclear staining of Twist (*a*,*d*) is decreased and delocalized compared to the NS Ctl. Twist suppression shows decreased and disrupted Glu (*b*,*e*) organization while vimentin (*c*,*f*) remained relatively unaffected. **C:** Live, detached MDA-MB-157s scored blindly following siTwist transfection displayed significantly lower McTN frequencies than NS ctl cells. *Columns*, mean for six experiments, in which at least 100 CellMask stained cells were counted; *bars*, SD. ($P \leq 0.05$, *T*-test, *black asterisks*).

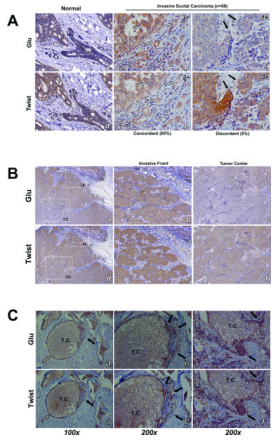

Figure 4. Immunohistochemical staining shows high concordance between Twist and Glu expression in patient tumor samples (33 patients; 66 samples)

A: Duplicate tissue microarrays stained for Glu and Twist were scored by intensity (negative, 0; weak, 1; moderate, 2; and strong, 3). Normal breast epithelial ducts (**N**) stain weakly for both Twist and Glu while the cancerous region (**C**) stains strongly (*a*,*d*). Patients with invasive ductal carcinoma exhibited high concordance (95%) between staining intensity and localization of Twist and Glu expression (*b*,*e*; white arrows). Discordance was observed in only 5% of patient samples (*c*,*f*; black arrows). Representative immunohistochemical scores are displayed in upper right corner. **B:** Low magnification shows an increase in staining intensity of Twist and Glu at the invasive front (**IF**) compared to the tumor center (**TC**) (*a*,*b*). Higher magnification shows stronger staining of Twist and Glu at the invasive front (*b*,*e*) while the tumor center stains weaker (*c*,*f*). **C:** Ductal carcinoma in situ (DCIS) samples *(a,b)* show weak expression of Twist and Glu in the tumor center enclosed by basement membrane (white arrows), but that both Twist and Glu are coordinately upregulated at sites of tumor invasion where the basement membrane is compromised (black arrows). Higher magnification image pairs *(b,e and c,f)* show Twist and Glu are upregulated in matching cells (black arrows).

NIH-PA Author Manuscript
NIH-PA Author Manuscript
NIH-PA Author Manuscript

NIH-PA Author Manuscript

NIH-PA Author Manuscript

NIH-PA Author Manuscript

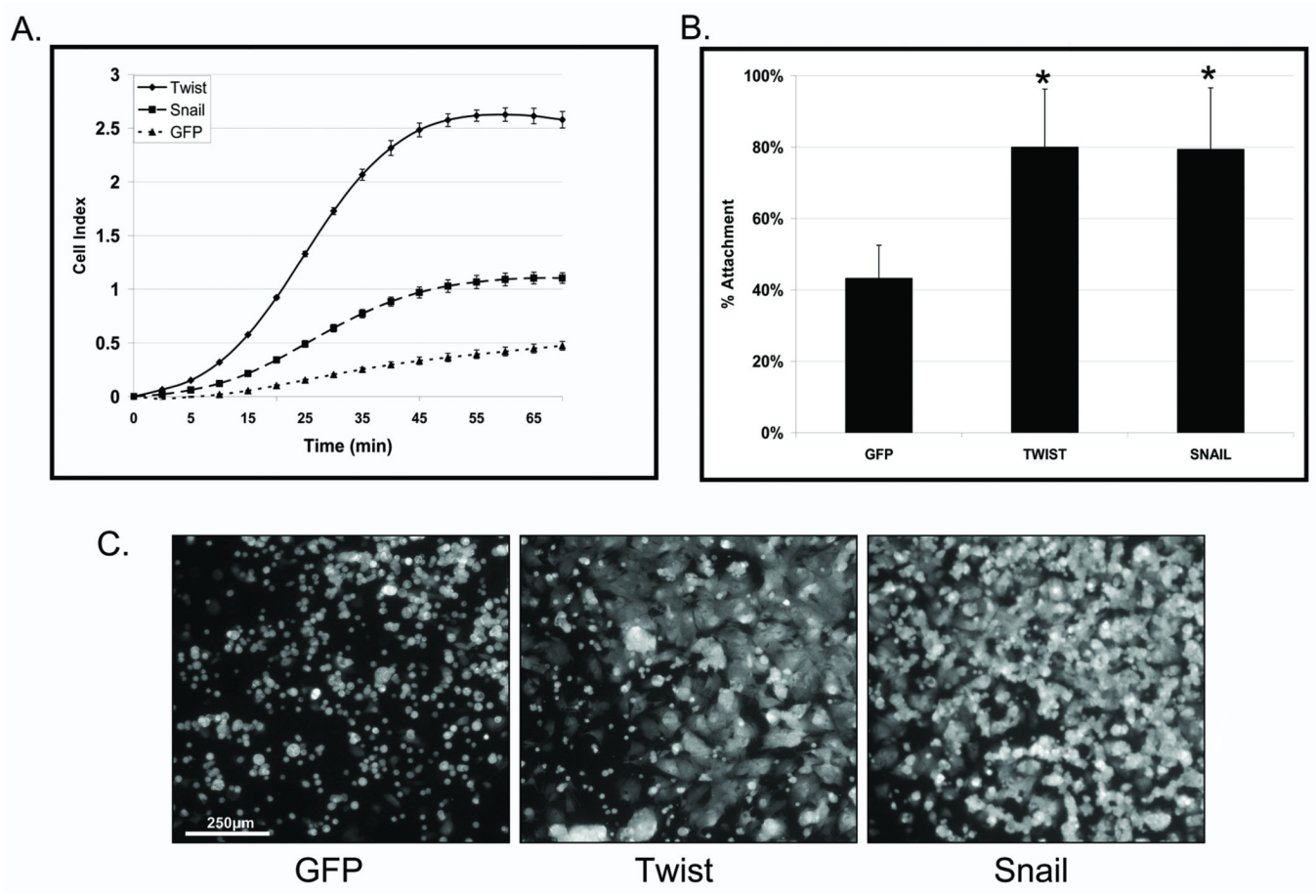

Figure 5. HMLE Twist and Snail have increased reattachment rates

A: HMLE Twist (—◆—) and Snail (- ■ -) lines attached at significantly faster rates then the HMLE-GFP (···▲···), as gauged by electrical impedence expressed as increasing cell index (CI). *Lines*, mean for 3 triplicate wells; *bars*, SD; representative graph shown. Three independent experiments were performed (Figure S4). **B:** CalceinAM-labeled HMLE Twist and Snail cells attach significantly more to confluent human bone marrow endothelial layers (HBME) at 1h than the HMLE-GFP cells (P≤0.005; *T*-test; *black asterisks*). *Columns*, mean for eight experiments; *bars*, SD. **C)** Representative images of calcein-AM labeled HMLEs over a confluent HBME layers.

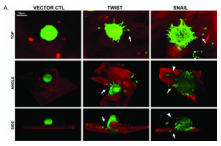

Figure 6. Microtentacles facilitate HMLE-endothelial attachment

A: Confocal imaging of GFP-Membrane transfected HMLE cells suspended for 20min over a confluent layer of mCherry-labeled HBME. Top, angle, and side views of HMLE cells at the early stages of attachment show HMLE-GFP vector control cells rounded without observable McTNs. HMLE-Twist displays a McTN anchoring to the top of the HBME (*white arrow*). HMLE-Snail exhibits McTNs extending under (*white arrow*) or bending towards (*white arrowheads*) the HBME layer.

NIH-PA Author Manuscript
NIH-PA Author Manuscript
NIH-PA Author Manuscript